Acta Mech 228, 3403–3419 (2017)
DOI 10.1007/s00707-017-1880-x

ORIGINAL PAPER

Petr Tovstik · Tatiana Tovstik

An elastic plate bending equation of second-order accuracy

Received: 23 January 2016 / Revised: 24 February 2017 / Published online: 17 June 2017

Abstract A study is carried out of a thin plate of constant thickness made of linearly elastic material which is transversally isotropic and heterogeneous in the thickness direction. Asymptotic expansions in powers of the relative plate thickness are constructed, and the bending equation of second-order accuracy (the SA model) is delivered. The results of the SA model are compared with the Kirchhoff–Love classical model and with the Timoshenko–Reissner (TR) model, as well as with the exact solution. To this end, some problems for a functionally gradient plate bending, and for a multi-layer plate bending and free vibration are solved and analysed. The range of plate heterogeneity, for which the error of the approximate models is small, is established. The TR model and the SA model are proved to yields results close to each other and the exact results for a very broad range of heterogeneity. That is why the generalized TR model for one-layered homogeneous transversely isotropic plate is proposed. Parameters of this model are chosen so that the results are close to the exact results and the results by the SA model. For the Navier boundary conditions, the analytical solution of 3D problems for a rectangular heterogeneous plate is constructed.

1 Introduction

The classical equation of the plate vibration was first derived by Marie-Sophie Germain in 1808 for explanation of the Chladni figures. The equation describing plate bending as well as plate vibration can be obtained on the basis of the Kirchhoff–Love (KL) hypotheses, cf. [1,2]. The equations accounting for the transversal shear follow from the Timoshenko–Reissner (TR) hypotheses [3,4] and present more sophisticated and exact variant of the plate theory.

Two-dimensional models of plates and shells are usually derived from the three-dimensional equations of elasticity theory. The above-mentioned KL and TR models can be considered as examples of constructing 2D models. Some other approaches are worth mentioning. The methods of expansions in series in terms of the Legendre polynomials in the thickness direction were suggested in [5]. A number of investigations, e.g. [6–9], are devoted to derivation of 2D equations by using asymptotic expansions in power series in terms of the small parameter $\mu = h/L$ which is the dimensionless plate thickness (h and L are the thickness and the typical wave length in the tangential directions, respectively). The other possibility, see, for example, [10,11], is a direct derivation of 2D equations of plates and shells without referring to 3D media.

In the present paper, we discuss the plate models (mainly the KL and the TR models) and their accuracy under various assumptions about material and structure of the plate. The asymptotic accuracy of the approach will be estimated by means of comparison with the 3D test problems which have exact solutions. These problems are equilibrium problems of infinite plates under a double periodic load. These three-dimensional problems are reduced to one-dimensional problems in z and have closed-form simple solutions.

P. Tovstik · T. Tovstik (✉)
Institute of Problems of Mechanical Engineering, St. Petersburg, Russia
E-mail: tovstik_t@mail.ru

The KL model is known to be asymptotically correct for an isotropic homogeneous plate, cf. [8]. This model yields the results of first-order accuracy with respect to the small thickness parameter μ. In contrast, the TR model turns out to be asymptotically incorrect for the isotropic homogeneous plates. This model is not more accurate than the KL model and does not include all second-order summands. Also, the TR model results in a differential equation of sixth order (in contrast to the differential equation of fourth order for KL model), and their solutions also describe the boundary layer effects. In 2D model, the boundary layer is not consistent with 3D stress–strain state (SSS). The boundary layer problem is discussed in Refs. [8,12,13] for some assumptions.

The difference between the KL and TR models becomes essential for orthotropic plate with a small shear stiffness, cf. [7,8,14]. If we introduce a shear parameter $g = \mu^2 E/G$ where E and G are the Young modulus and the transversal shear modulus, respectively, then for $g \sim 1$, the KL model is inapplicable, while the TR model yields sufficiently accurate results.

The problem of a general anisotropy with 21 elastic moduli is essentially more challenging. As shown in Refs. [12,15,16], the KL model and the standard TR model are inconsistent in the principal terms with respect to μ. In this case, the generalized TR model leads to a system of differential equations of sixth order, and the problem of excluding the boundary layer arises, see [12,15]. By using asymptotic expansions [17], one obtains a system of fourth order (as in the KL model). Various problems for plate with a general anisotropy are discussed in Refs. [18,19]. A benchmark of various plate models can be found in Refs. [7,20–25]. General problems of the plate theory are described in books [18,26–29]. The heterogeneous (or functionally graded in the thickness direction) plates and, in particular, the multi-layered and laminated plates are studied in a number of works [5,7,21,30–35]. A number of works are devoted to the problems of plate vibration, e.g. [36–40]. The general asymptotic theory of laminated plates with two small parameters is presented in [48].

The present paper is concerned with the study of a thin plate of constant thickness made of a linearly elastic material which is transversally isotropic and heterogeneous in the thickness direction. For the transversally isotropic material, it is possible to split the 3D system of sixth order of the elasticity theory into two systems of second and fourth order, see [41]. However, this is not the case for the orthotropic plate and the plate with general anisotropy. Asymptotic expansions in powers of the small thickness parameter μ are constructed, and the bending equation of the second-order accuracy (the SA model, for short) is obtained. The present paper is inspired by paper [42], in which an isotropic homogeneous plate is studied, and paper [7], in which a heterogeneous plate is briefly examined. The results of the SA model are compared with the KL classical model and the TR model and also with the exact numerical solution. To this end, the numerical examples for a functionally gradient plate bending, for a multi-layer plate bending and free vibrations are studied. It allows us to establish the range of plate heterogeneity for which the error of the approximate models is small. It is shown that the TR model and the SA model gives results close to each other and to the exact results for a very wide range of heterogeneity. This is a reason for applying the generalized TR model for single-layered homogeneous transversely isotropic plate. The model parameters are chosen so that the obtained results are close to the exact solution and to the results of the SA model. The analytical solution of 3D problems for the rectangular heterogeneous plate is constructed for the Navier boundary conditions.

2 Equilibrium equations and the simplification

Consider the problem of bending of a thin plate made of a transversally isotropic heterogeneous material. The 3D equilibrium equations are

$$\frac{\partial \sigma_{ij}}{\partial x_j} + f_i = 0, \qquad i, j = 1, 2, 3, \qquad 0 \le x_3 = z \le h, \tag{1}$$

where x_j are the Cartesian coordinates, f_i are the projections of the external load intensity, and the summation is carried out over repeating subscripts.

The stresses are related to the strains as follows:

$$\begin{aligned}
&\sigma_{11} = E_{11}\varepsilon_{11} + E_{12}\varepsilon_{22} + E_{13}\varepsilon_{33}, && \sigma_{12} = G_{12}\varepsilon_{12},\\
&\sigma_{22} = E_{12}\varepsilon_{11} + E_{11}\varepsilon_{22} + E_{13}\varepsilon_{33}, && \sigma_{13} = G_{13}\varepsilon_{13},\\
&\sigma_{33} = E_{13}\varepsilon_{11} + E_{13}\varepsilon_{22} + E_{33}\varepsilon_{33}, && \sigma_{23} = G_{13}\varepsilon_{23},\\
&\varepsilon_{11} = \frac{\partial u_1}{\partial x_1}, \qquad \varepsilon_{12} = \frac{\partial u_1}{\partial x_2} + \frac{\partial u_2}{\partial x_1}, && \text{etc.},
\end{aligned} \tag{2}$$

with $E_{11} = E_{12} + 2G_{12}$. Here u_1 and u_2 denote the displacements in the corresponding directions. The elastic moduli E_{ij}, G_{ij} do not depend on the tangential coordinates x_1, x_2, but they can depend on the transversal coordinate $x_3 = z$. For functionally gradient materials, the moduli are continuous functions in z, while for the multi-layered plates they are piecewise continuous functions.

For a transversally isotropic material, the moduli depend on the five elastic parameters $E,\ E',\ G_{13},\ \nu,\ \nu'$, e.g. [5]:

$$E_{11} = \frac{E\left(1-\nu'^2\right)}{(1+\nu)\left(1-\nu-2\nu'^2\right)}, \qquad E_{12} = \frac{E\left(\nu+\nu'^2\right)}{(1+\nu)\left(1-\nu-2\nu'^2\right)}, \qquad G_{12} = G = \frac{E}{2(1+\nu)},$$
$$E_{13} = \frac{E\nu'}{1-\nu-2\nu'^2}, \qquad E_{33} = \frac{E'(1-\nu)}{1-\nu-2\nu'^2}, \qquad G_{13} = G'. \tag{3}$$

For the isotropic material, $E' = E$, $\nu' = \nu$, where E and ν are the Young's modulus and the Poisson ratio, respectively.

We set the homogeneous boundary conditions on the face planes $z = 0$ and $z = h$:

$$\sigma_{i3} = 0, \quad i = 1, 2, 3. \tag{4}$$

If the surface forces are given, then they are included in the body forces by using the Dirac's delta function.

Let us introduce the new unknown functions u, v, σ, τ as

$$u = \frac{\partial u_1}{\partial x_1} + \frac{\partial u_2}{\partial x_2}, \qquad v = \frac{\partial u_1}{\partial x_2} - \frac{\partial u_2}{\partial x_1},$$
$$\sigma = \frac{\partial \sigma_{13}}{\partial x_1} + \frac{\partial \sigma_{23}}{\partial x_2}, \qquad \tau = \frac{\partial \sigma_{13}}{\partial x_2} - \frac{\partial \sigma_{23}}{\partial x_1}. \tag{5}$$

For the transversally isotropic material the system (1), (2) is split into two sub-systems, cf. [42]:

$$\frac{\partial \tau}{\partial z} + G_{12}\Delta v + m_1 = 0, \quad \tau = G_{13}\frac{\partial v}{\partial z}, \quad \Delta = \frac{\partial^2}{\partial x_1^2} + \frac{\partial^2}{\partial x_2^2}, \quad m_1 = \frac{\partial f_1}{\partial x_2} - \frac{\partial f_2}{\partial x_1}. \tag{6}$$

$$\sigma_{33} = E_{13}u + E_{33}\frac{\partial w}{\partial z}, \quad \sigma = G_{13}\left(\frac{\partial u}{\partial z} + \Delta w\right), \qquad w = u_3,$$
$$\frac{\partial \sigma}{\partial z} + E_0\Delta u + \frac{E_{13}}{E_{33}}\Delta\sigma_{33} + m = 0, \quad \frac{\partial \sigma_{33}}{\partial z} + \sigma + f_3 = 0, \quad m = \frac{\partial f_1}{\partial x_1} + \frac{\partial f_2}{\partial x_2}, \tag{7}$$

with

$$E_0 = E_{11} - \frac{E_{13}^2}{E_{33}} = \frac{E}{1-\nu^2}.$$

The system (6) of differential equations of the second order in z describes the boundary layer.

System (7) of the fourth order describes the plate bending, and the 2D plate model is obtained here by using asymptotic expansions [7,14]. The asymptotic solution is based on the expansions in powers of the small parameter $\mu = h/L$.

We introduce the dimensionless variables (denoted by $\hat{}$)

$$\{u_1, u_2, w, z\} = h\left\{\hat{u}_1, \hat{u}_2, \hat{w}, \hat{z}\right\}, \quad \{x_1, x_2\} = L\left\{\hat{x}_1, \hat{x}_2\right\}, \quad u = \mu\hat{u}, \quad \sigma = \frac{E_*}{L}\hat{\sigma},$$
$$\{\sigma_{ij}, E_{ij}, G_{ij}, E_0\} = E_*\left\{\hat{\sigma}_{ij}, \hat{E}_{ij}, \hat{G}_{ij}, c_0\right\}, \quad f_i = \frac{E_*}{h}\hat{f}_i, \quad E_* = \frac{1}{h}\int_0^h E_0(z)\mathrm{d}z, \tag{8}$$

and rewrite the system (7) in dimensionless form:

$$\frac{\partial \hat{w}}{\partial \hat{z}} = -\mu c_\nu \hat{u} + c_3\hat{\sigma}_{33}, \qquad \frac{\partial \hat{u}}{\partial \hat{z}} = -\mu\hat{\Delta}\hat{w} + c_g\hat{\sigma},$$
$$\frac{\partial \hat{\sigma}}{\partial \hat{z}} = Y_3(\hat{z}) = -\mu^2 c_0\hat{\Delta}\hat{u} - \mu c_\nu\hat{\Delta}\hat{\sigma}_{33} - \hat{m}, \quad \frac{\partial \hat{\sigma}_{33}}{\partial \hat{z}} = Y_4(\hat{z}) = -\mu\hat{\sigma} - \hat{f}_3, \quad 0 \le \hat{z} \le 1, \tag{9}$$

with

$$c_\nu = \frac{E_{13}}{E_{33}} = \frac{\nu}{1-\nu}, \quad c_3 = \frac{E_*}{E_{33}}, \quad c_g = \frac{E_*}{G_{13}},$$
$$\hat\sigma = \frac{\partial\hat\sigma_{13}}{\partial\hat x_1} + \frac{\partial\hat\sigma_{23}}{\partial\hat x_2}, \quad \hat m = \frac{\partial\hat f_1}{\partial\hat x_1} + \frac{\partial\hat f_2}{\partial\hat x_2}, \quad \hat\Delta = \frac{\partial^2}{\partial\hat x_1^2} + \frac{\partial^2}{\partial\hat x_2^2}. \tag{10}$$

Here L is a representative wave length in the in-plane directions and E_* is the average value of modulus E_0. The dimensionless coefficients c_0, c_ν, c_g, c_3 are given functions of $\hat z$. The boundary conditions (4) yield

$$\hat\sigma = \hat\sigma_{33} = 0 \quad \text{at} \quad \hat z = 0,\ \hat z = 1. \tag{11}$$

In what follows, the hat sign will be omitted.

3 Asymptotic solution of boundary value problem (9), (11) in the static case

Assume that the dimensionless external forces f_3, m are of the order of unity. Then, the orders of the plate quantities are as follows:

$$\sigma_{33} = O(1), \quad \sigma = O\left(\mu^{-1}\right), \quad u = O\left(\mu^{-3}\right), \quad w = O\left(\mu^{-4}\right). \tag{12}$$

These estimates correspond to the standard KL model, that is, which $\sigma = \mu\, O(\sigma_{ij})$ and $\sigma_{33} = \mu^2 O(\sigma_{ij})$, where $\sigma_{ij},\ i, j = 1, 2$, are the in-plane stresses, and σ, Eq. (5) describes the transversal shear stresses. The stresses $\sigma_{ij},\ i, j = 1, 2$, are excluded from Eqs. (1) and (2) with the help of new unknown functions (5).

The right-hand sides in Eq. (9) are small, and it allows one to apply the method of iterations [7,14]. To construct the solution of second-order accuracy, we take

$$w = \mu^{-4}w_0 + \mu^{-2}w_2, \quad u = \mu^{-3}u_0 + \mu^{-1}u_2, \quad \sigma = \mu^{-1}\sigma_0 + \mu\sigma_2, \quad \sigma_{33} = \sigma_{33,0} + \mu^2\sigma_{33,2}. \tag{13}$$

The arbitrary functions $w^c(x_1, x_2)$ and $u^c(x_1, x_2)$ appear after integration of the first two equations (9) with respect to z. These functions are obtained from the compatibility conditions of two remaining equations (9) and the boundary condition (11)

$$\langle Y_3(z)\rangle = 0, \quad \langle Y_4(z)\rangle = 0, \qquad \langle Z(z)\rangle \equiv \int_0^1 Z(z)\mathrm{d}z. \tag{14}$$

In the zero approximation, we obtain

$$w_0 = w_0(x_1, x_2), \quad u_0 = (a - z)\Delta^2 w_0, \quad a = \langle z c_0(z)\rangle,$$
$$\sigma_0 = \varphi_1(z)\Delta^2 w_0, \quad \varphi_1(z) = \int_0^z c_0(z)(z - a)\mathrm{d}z,$$
$$D\Delta^2 w_0 = F_3, \qquad D = \left\langle (z - a)^2 c_0(z)\right\rangle, \quad F_3 = \langle f_3(z)\rangle,$$
$$\sigma_{33,0} = -\frac{F_3}{D}\varphi_2 - \varphi_3, \quad \varphi_2(z) = \int_0^z \varphi_1(z)\mathrm{d}z, \quad \varphi_3(x_1, x_2, z) = \int_0^z f_3(x_1, x_2, z)\mathrm{d}z, \tag{15}$$

where $z = a$ is the position of the plate neutral layer, D is the bending stiffness of the plate with changing elastic moduli, F_3 is the overall transversal force. The equation $D\Delta^2 w_0 = F_3$ corresponds to the classic KL model. The function w_0 does not depend on z, but the small stress $\sigma_{33,0}$ depends on the distribution of function $f_3(z)$ in the thickness direction ($\sigma_{33} = 0$ for the KL model).

In the second approximation, the solution is more bulky. Here we show only function w_2 which is a function of z. At $z = 0$, it satisfies the equation

$$D\Delta^2 w_2(0) = A\Delta F_3 + L(\Delta f_3) - M, \tag{16}$$

where

$$A = A_g - A_\nu, \quad L(\Delta f_3) = \int_0^1 c_\nu(z)(a - z)\left(\int_0^z \Delta f_3 \mathrm{d}z_1\right)\mathrm{d}z, \quad M = \int_0^1 (a - z)m(z)\mathrm{d}z,$$

$$A_g = \frac{1}{D}\int_0^1 c_0(z)(z-a)\int_0^z c_g(z_1)\int_0^{z_1} c_0(z_2)(z_2-a)\mathrm{d}z_2\mathrm{d}z_1\mathrm{d}z,$$
$$A_\nu = \frac{1}{D}\int_0^1 (z-a)\left(c_\nu(z)\int_0^z\int_0^{z_1} c_0(z_2)(z_2-a)\mathrm{d}z_2\mathrm{d}z_1 + c_0(z)\int_0^z\int_0^{z_1} c_\nu(z_2)(z_2-a)\mathrm{d}z_2\mathrm{d}z_1\right)\mathrm{d}z. \quad (17)$$

The total deflection of the reference plane $z = 0$ satisfies the equation

$$D\mu^4\Delta^2 w(0) = F_3 + \mu^2(A\Delta F_3 + L(\Delta f_3) - M) + O(\mu^4), \quad (18)$$

in which the coefficients D and A depend on the elastic moduli distribution in the plate thickness, and the summands $L(\Delta f_3)$ and M depend on the distribution of external transversal and tangential loads, respectively. The coefficients A_g and A_ν take into account the transversal shear and the Poisson ratio, respectively.

The total deflection $w(z)$ of the arbitrary plane z is expressed in terms of $w(0)$ as

$$w(z) = w(0) + \mu^2\Delta w(0)\int_0^z c_\nu(z)(z-a)\mathrm{d}z. \quad (19)$$

If the plate is loaded only by an external surface normal pressure F_3 acting on the plane $z = 0$, then $L(\Delta f_3) = \langle c_\nu(a-z)\rangle\,\Delta F_3$ and $M = 0$ in Eq. (18); hence, Eq. (18) takes the form

$$D\mu^4\Delta^2 w(0) = F_3 + \mu^2 A_1\Delta F_3, \quad A_1 = A + \int_0^1 c_\nu(z)(z-a)\mathrm{d}z. \quad (20)$$

Remark 1 If the plate is homogeneous, then the elastic moduli c_0, c_g, c_ν are constant, the integrals (17) are calculated, and Eq. (20) yields

$$D\mu^4\Delta^2 w(0) = F_3 + \mu^2 A_1\Delta F_3, \quad A_1 = \frac{2c_\nu - c_g}{10}, \quad D = \frac{1}{12}. \quad (21)$$

For a homogeneous plate $a = 1/2$, i.e. the neutral plane can be understood as a reference plane, and we obtain from Eq. (19)

$$D\mu^4\Delta^2 w(1/2) = F_3 + \mu^2 A_2\Delta F_3, \quad A_2 = \frac{3c_\nu - 4c_g}{40}, \quad (22)$$

and for the isotropic plate we have $A_2 = (3\nu - 8)/(40(1-\nu))$. This value A_2 was obtained in [46], where it was noted that the authors of Refs. [4,20,28] also derived Eq. (22); however, they obtained the values of A_2 that differ from the values presented above.

Equations (18)–(20) describe the internal solution. The boundary conditions at the plate edges and the possible boundary layer effects near the edges are ignored. The question thus arises as to how to choose the typical wave length L that appears in the relation $\mu = h/L$. There is a harmonic problem in which the value L can be defined (see Remark 2).

Remark 2 Let the external loads be the harmonic functions of x_1, x_2:

$$f_3(x_1, x_2, z) = f_3^0(z)\sin(r_1x_1)\sin(r_2x_2), \quad m(x_1, x_2, z) = m^0(z)\sin(r_1x_1)\sin(r_2x_2). \quad (23)$$

Then, the internal solution $w(x_1, x_2, z) = w^0(z)\sin(r_1x_1)\sin(r_2x_2)$ and the other unknown functions in Eqs. (9) are harmonic functions, too, and $\Delta w = -(r_1^2 + r_2^2)w$. Therefore, if we put (in the initial designations)

$$L = \left(r_1^2 + r_2^2\right)^{-1/2}, \quad (24)$$

then according to the definition of small parameter $\mu = h/L$ the Laplace operator Δ can be replaced by -1 in all formulae in Sect. 3.

Applications of Eqs. (18)–(20) for rectangular plates are discussed in Sect. 8.

4 Free vibrations

The equation for the low-frequency free vibrations is derived here by means of the results of Sect 3. We augment Eqs. (1) with the inertia term

$$f_i = \rho(x_3)\omega^2 u_i, \quad i = 1, 2, 3, \tag{25}$$

where ω is the natural frequency and $\rho(x_3)$ is the mass density. Then, in Eq. (9)

$$f_3 = \lambda w(x_1, x_2, z)\rho_0(z), \quad m = \lambda u(x_1, x_2, z)\rho_0(z), \tag{26}$$

with

$$\lambda = \frac{\rho_* h^2\omega^2}{E_*}, \quad \rho_0(z) = \frac{\rho(z)}{\rho_*}, \quad \rho_* = \frac{1}{h}\int_0^h \rho(z)\mathrm{d}z. \tag{27}$$

Here λ is the frequency parameter depending on the average values of the mass density ρ_* and elastic modulus E_* (see Eq. (8)).

We express all the summands of Eq. (18) in terms of $w(x_1, x_2, 0)$:

$$\begin{aligned} F_3 &= \lambda\left(w(x_1, x_2, 0) + \mu^2\Delta w(x_1, x_2, 0)\int_0^1\int_0^z c_\nu(z)\rho_0(z_1)(z_1 - a)\mathrm{d}z_1\,\mathrm{d}z\right), \\ L(\Delta f_3) &= \lambda\Delta w(x_1, x_2, 0)\int_0^1 c_\nu(z)(a - z)\int_0^z \rho_0(z_1)\mathrm{d}z_1\,\mathrm{d}z, \\ M &= \lambda\Delta w(x_1, x_2, 0)\int_0^1 (a - z)^2\rho_0(z)\mathrm{d}z. \end{aligned} \tag{28}$$

Now Eq. (18) takes the form

$$D\mu^4\Delta^2 w(x_1, x_2, 0) = \lambda\left(w(x_1, x_2, 0) + \mu^2(A_g - A_\nu + A_\rho)\Delta w(x_1, x_2, 0) + O\left(\mu^4\right)\right), \tag{29}$$

where the summands A_g and A_ν are the same as in Eq. (17) and the summand A_ρ depends on the distribution of mass density in the thickness direction

$$A_\rho = \int_0^1 \left((z - a)^2\rho_0(z) - \rho_0(z)\int_0^z c_\nu(z_1)(z_1 - a)\mathrm{d}z_1 + c_\nu(z)(z - a)\int_0^z \rho_0(z_1)\mathrm{d}z_1\right)\mathrm{d}z. \tag{30}$$

Let the function $w(x_1, x_2, 0)$ in Eq. (18) be harmonic. Then, according to Remark 2 the formal substitution $\Delta = -1$ yields

$$\lambda = D\mu^4\left(1 - \mu^2(A_g - A_\nu - A_\rho) + O\left(h_*^4\right)\right)^{-1}. \tag{31}$$

Formula (31) is valid not only for deflections $w(x_1, x_2) = w^0\sin(r_1x_1)\sin(r_2x_2)$ with $r_1^2 + r_2^2 = 1$, but also for any deflections satisfying Helmholtz's equation $\Delta w + w = 0$.

Remark 3 In the case of a homogeneous plate, Eq. (31) can be simplified to give

$$\lambda = \frac{\mu^4}{12}\left(1 + \mu^2\left(\frac{1}{12} + \frac{c_g}{10} + \frac{c_\nu}{30} + O\left(\mu^4\right)\right)\right)^{-1}. \tag{32}$$

It follows from the latter equation that the frequency depends on the elasticity parameters c_g and c_ν and the thickness-wave parameter $\mu = h\sqrt{r_1^2 + r_2^2}$ rather than on each of the wave numbers r_1 and r_2 alone.

In Sects. 5 and 6 for some partial cases, the accuracy of asymptotic formulae (18) and (31) is estimated by comparison with the numerical solutions of Eq. (9).

5 Deflection of a plate made of a transversely isotropic heterogeneous material

The elasticity relations (3) are not convenient for our aim because modulus G_{13} is independent of the other moduli. Consider the two-parametric set of transversely isotropic materials introduced in [42]:

$$E_0 = \frac{E}{1-\nu^2}, \quad E_{33} = \frac{4(1-\nu)^2\eta E_0}{(1+\eta)^2(1-2\nu)}, \quad G_{13} = \frac{2(1-\nu)\eta E_0}{(1+\eta)^2}, \quad c_\nu = \frac{\nu}{1-\nu}. \tag{33}$$

This material can be obtained as a limit of the multi-layered material with the alternating isotropic layers with parameters E_1, ν_1, h_1 and E_2, ν_2, h_2 under the assumption that

$$E = \frac{E_1+E_2}{2}, \quad \nu_1 = \nu_2 = \nu, \quad \eta = \frac{E_2}{E_1} \le 1, \quad h_1 = h_2 \to 0. \tag{34}$$

Here E_1 and E_2 are the Young's moduli of the layers, E is the average Young's modulus, ν is the Poisson ratio, and η is the measure of anisotropy. The material is isotropic provided that $\eta = 1$. If $\eta \ll 1$ the material is strongly anisotropic and soft in the transversal direction because the moduli E_{33}, G_{13} are small.

Assume that for the studied functionally gradient material $E_0 = E_0(z)$ is a prescribed function of z, whereas the parameters η and ν do not depend on z. Similar to Eq. (8), we put $E_0(z) = E_* c_0(z)$, $\langle c_0(z)\rangle = 1$; then,

$$E_{33}(z) = e_{33}c_0(z), \quad G_{13} = g c_0(z), \quad e_{33} = \frac{4(1-\nu)^2\eta}{(1+\eta)^2(1-2\nu)}, \quad g = \frac{2(1-\nu)\eta}{(1+\eta)^2}, \tag{35}$$

where the function $c_0(z)$ describes the elastic properties distribution in the thickness direction.

Let the load be a normal pressure F_3 in plane $z = 0$. Then, the coefficients D and A_1 in Eq. (20) are as follows:

$$D = \left\langle (z-a)^2 c_0(z)\right\rangle, \quad a = \langle z c_0(z)\rangle, \quad A_1 = c_g\psi_g + c_\nu\psi_c, \quad c_g = 1/g, \tag{36}$$

$$\psi_g = \frac{1}{D}\left\langle (z-a)c_0(z)\int_0^z \frac{1}{c_0(z_1)}\left(\int_0^{z_1}(z_2-a)c_0(z_2)\mathrm{d}z_2\right)\mathrm{d}z_1\right\rangle,$$

$$\psi_c = \frac{1}{D}\left\langle (a-z)\left(\int_0^z\left(\int_0^{z_1}(z_2-a)c_0(z_2)\mathrm{d}z_2\right)\mathrm{d}z_1 + c_0(z)\int_0^z\left(\int_0^{z_1}(z_2-a)\mathrm{d}z_2\right)\mathrm{d}z_1 + 1\right)\right\rangle. \tag{37}$$

The constants a, D, ψ_g, ψ_c depend on heterogeneity of the elastic moduli in the thickness direction. If $c_0 = 1$, then

$$a = \frac{1}{2}, \quad D = \frac{1}{12}, \quad \psi_c = \frac{1}{5}, \quad \psi_g = -\frac{1}{10}, \tag{38}$$

and so we return to Eq. (21).

Consider the case $c_0(z) = \alpha e^{\alpha z}/(e^\alpha - 1)$. Estimation of the integrals in Eq. (37) gives

$$a(\alpha) = \frac{\alpha-1}{\alpha} + \frac{1}{e^\alpha - 1}, \quad D(\alpha) = \frac{(e^\alpha-1)^2 - \alpha^2 e^\alpha}{\alpha^2(e^\alpha-1)^2},$$

$$\psi_g(\alpha) = \frac{2(1-e^{3\alpha}) + (\alpha^3-6)e^\alpha + (\alpha^3+6)e^{2\alpha}}{\alpha^2(e^\alpha-1)((e^\alpha-1)^2 - \alpha^2 e^\alpha)}, \tag{39}$$

$$\psi_c(\alpha) = (a(\alpha) - 1/2)/D + \frac{6\alpha^3 e^\alpha(e^\alpha+1) + 3\alpha^2(e^\alpha+1)^2(e^\alpha-1) - 6\alpha(e^\alpha+1)(e^\alpha-1)^2 - \alpha^4 e^\alpha(e^\alpha-1) - 12(e^\alpha-1)^3}{6\alpha^2(e^\alpha-1)((e^\alpha-1)^2 - \alpha^2 e^\alpha)}.$$

The plots of the functions (39) are shown in Fig. 1. At $\alpha \to 0$, these functions approach the values (38).

To estimate the accuracy of the approximate models, we compare the exact value $w(0)$ from Eqs. (9) and approximate asymptotic values. Assume that the load $F_3(x_1, x_2)$ is harmonic, i.e. $F_3(x_1, x_2) = F_3^0 \sin(r_1 x_1)\sin(r_2 x_2)$. According to Remark 2, Eqs. (9) become ordinary differential equations with $\mu^2 = h^2(r_1^2 + r_2^2)$.

For numerical work, we take $\mu = 0.2$, $\nu = 0.3$, and compare the isotropic material $\eta = 1$ and the materials with three levels of anisotropy $\eta = 0.1,\ 0.01,\ 0.001$. We study the homogeneous material ($\alpha = 0$) and two

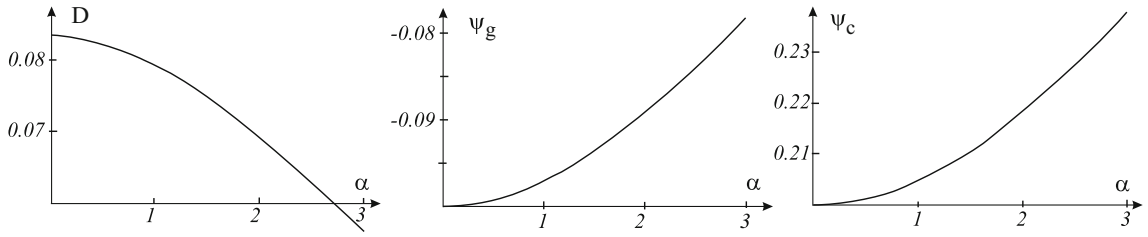

Fig. 1 Functions $D(\alpha)$, $\psi_g(\alpha)$, $\psi_c(\alpha)$

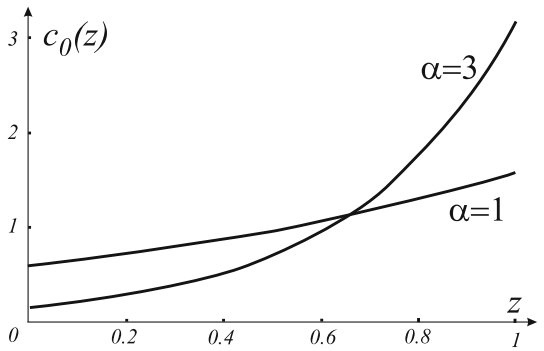

Fig. 2 Functions $c_0(z)$ at $\alpha = 1$ and $\alpha = 3$

Table 1 Errors of the approximate models depending on the level of the plate anisotropy (η) and heterogeneity (α)

η	c_g	α	w^{exact}	w^{KL}	e^{KL} (%)	w^{TR}	e^{TR} (%)	w^{SA}	e^{SA} (%)
1	2.86	0	6880	6825	0.8	6903	0.3	6880	0.01
		1	7215	7170	0.6	7249	0.5	7224	0.01
		3	10,174	10,162	0.1	10,252	0.8	10,211	0.4
0.1	8.64	0	7038	6825	3	7061	0.3	7038	0.01
		1	7385	7170	3	7410	0.5	7385	0.01
		3	10,361	10,162	2	10,437	0.8	10,396	0.3
0.01	72.86	0	8782	6825	22	8814	0.3	8791	0.1
		1	9107	7170	22	9200	0.4	9174	0.1
		3	12,412	10,162	18	12,482	0.6	12,440	0.2
0.001	715.7	0	25,902	6825	74	26,364	1.8	26,341	1.7
		1	26,563	7170	73	7107	2.1	27,082	1.9
		3	31,777	10,162	64	32,953	3.7	32,912	3.6

heterogeneous materials with $\alpha = 1$ and $\alpha = 3$. The graphs of the function $c_0(z) = \alpha e^{\alpha z}/(e^{\alpha} - 1)$ describing the variation are shown in Fig. 2.

In order to compare the exact and the approximate values of deflections, it is enough to take $F_3 = 1$ and $E_* = 1$ since the problem is linear. Table 1 displays the exact values w^{exact} and the functions

$$w^{\text{KL}} = \frac{F_3}{\mu^4 D}, \quad w^{\text{TR}} = \frac{F_3}{\mu^4 D}\left(1 - \mu^2 c_g \psi_g\right), \quad w^{\text{SA}} = \frac{F_3}{\mu^4 D}\left(1 - \mu^2 c_g \psi_g - \mu^2 c_v \psi_c\right). \tag{40}$$

Here and in what follows, w^{TR} denotes solution of the generalized TR model constructed in Sect. 7 rather than the solution of standard TR system of equations.

Here the error of the approximate models e^{KL}, e^{TR}, e^{SA} is defined as follows: $e^a = (w^a - w^{\text{exact}})/w^a$ with $a = \{\text{KL,TR,SA}\}$.

The value w^{KL} corresponds to the KL model and gives the acceptable accuracy only for a small level of anisotropy. The correcting summand $\mu^2 c_g \psi_g$ in (40) takes into account the transversal shear deformation, and the summand $\mu^2 c_v \psi_c$ involves the deformation of normal fibres relating to the Poisson's effect. The value w^{SA} is asymptotically exact with the second-order accuracy if both summands are included. This is proved by the results shown in Table 1.

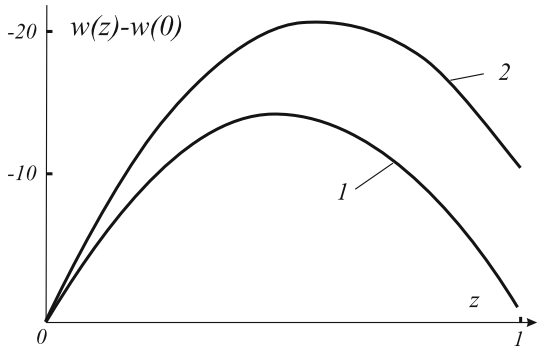

Fig. 3 Function $w(z) - w(0)$ for homogeneous (*1*) and for heterogeneous (*2*) materials

For small levels of anisotropy ($c_g \leq 10$), the Poisson effect makes the result essentially accurate (for the small heterogeneity, the error is of the order 0.01%), and for $\eta \sim 0.01{-}0.001$ the shear summand becomes principal, the Poisson effect being relatively small.

In Table 1, the deflection of the plane $z = 0$ is discussed. With the relative error of the order of μ^2, the deflection of the plane $z = 1$ can be determined from Eq. (19):

$$w(1) = w(0) + \mu^2 \Delta w(0) \int_0^1 c_\nu(z - a)\mathrm{d}z. \tag{41}$$

For more detailed discussion of this relation, we write down the expansion (13)

$$w(z) = \mu^{-4} w_0 + \mu^{-2} w_2(z) + w_4(z) + O(\mu^2), \tag{42}$$

The function w_0 does not depend on z (in the most approximate models $w = w(0) = \text{const.}$). The function w_2 depends on z, and for a homogeneous plate this function is even with respect to the midplane $z = 1/2$, and $w_2(1) = w_2(0)$. In the general case, $w_2(1) \neq w_2(0)$.

Figure 3 displays the variable part $w(z) - w_0$ of the functions $w(z)$ obtained by numerical solution of Eq. (9) for $\mu = 0.2$. Curve *1* is plotted for a homogeneous material while curve *2* is plotted for a heterogeneous material $c_0(z) = \alpha e^{\alpha z}/(e^\alpha - 1)$ with $\alpha = 1$. For curve *1*, we get $w(0) = 6880$, $w_2(0) = w_2(1)$, but $w(1) - w(0) = w_4(1) = -0.455$ [see Eq. (42)]. For $\mu = 0.1$, a calculation gives the same value $w(1) - w(0) = -0.455$ in spite of $w(0) = 6880 \cdot 2^4 = 110,080$.

For a heterogeneous material (see curve *2*), we have $w_2(0) \neq w_2(1)$ and $w(1) - w(0) = -9.5$. The difference $w(z) - w(0)$ is not symmetric with respect to $z = 1/2$, while for a homogeneous material it is nearly symmetric.

6 Deflections and vibrations of a multi-layered plate

Consider a plate of thickness h consisting of n homogeneous isotropic layers with thicknesses h_k, $k = 1, 2, ..., n$ ($h = \sum h_k$). Let E_k, ν_k, ρ_k be the Young's moduli, the Poisson ratios, and the mass densities of the layers, respectively. We set

$$z_0 = 0, \quad z_k = \sum_{i=1}^{k} h_i, \quad e_k = \frac{E_k}{1 - \nu_k^2}, \quad c_k = \frac{\nu_k}{1 - \nu_k}, \quad g_k = \frac{E_k}{2(1 + \nu_k)}. \tag{43}$$

The coordinate $z = a$ of the neutral layer, the bending stiffness D according to the KL model, and the coefficients A_g and A_ν in Eq. (17) are as follows:

$$a = \frac{1}{2} \sum_{k=1}^{n} e_k \left(z_k^2 - z_{k-1}^2\right) \left(\sum_{k=1}^{n} e_k h_k\right)^{-1}, \quad D = \frac{1}{3} \sum_{k=1}^{n} e_k \left(\hat{z}_k^3 - \hat{z}_{k-1}^3\right), \quad \hat{z}_k = z_k - a,$$

Table 2 Errors of the approximate models for some values of E_2

E_2	$w(0)^{\text{exact}}$	w^{KL}	e^{KL} (%)	w^{TR}	e^{TR} (%)	$w(0)^{\text{SA}}$	e^{SA} (%)
1	6290	6235	0.9	6323	0.5	6290	0.005
0.1	18,770	18015	4.0	18811	0.2	18769	0.006
0.01	31,802	23,900	24.8	31,815	0.04	31,803	0.003
0.001	103,135	24,852	75.9	104,073	0.9	104,069	0.9
0.0001	726,176	24,954	97.0	817,277	12.5	817,274	12.5

$$A_g = \frac{1}{D}\sum_{k=1}^{n}\left(\frac{e_k f_{1k}}{2}\left(\hat z_k^2 - \hat z_{k-1}^2\right) + \frac{f_{2k}}{3g_k}\left(\hat z_k^3 - \hat z_{k-1}^3\right) + \frac{e_k}{30g_k}\left(\hat z_k^5 - \hat z_{k-1}^5\right)\right),$$

$$A_\nu = \frac{1}{D}\sum_{k=1}^{n}\left(\frac{e_k f_{3k}^c + c_k f_{3k}^e}{2}\left(\hat z_k^2 - \hat z_{k-1}^2\right) + \left(c_k f_{4k}^e + e_k f_{4k}^c\right)\left(\hat z_k^3 - \hat z_{k-1}^3\right) + \frac{e_k c_k}{15}\left(\hat z_k^5 - \hat z_{k-1}^5\right)\right), \quad (44)$$

where

$$f_{1k} = \sum_{i=1}^{k-1}\left(\frac{f_{2i}h_i}{g_i} + \frac{e_i}{6g_i}\left(\hat z_i^3 - \hat z_{i-1}^3\right)\right) - \frac{f_{2k}h_k}{g_k} - \frac{e_k}{6g_k}\hat z_k^3, \quad f_{2k} = \frac{1}{2}\sum_{i=1}^{k-1} e_i\left(\hat z_i^2 - \hat z_{i-1}^2\right) - \frac{1}{2}e_k\hat z_k^2,$$

$$f_{3k}^e = \sum_{i=1}^{k-1}\left(f_{4i}^e h_i + \frac{e_i}{6}\left(\hat z_i^3 - \hat z_{i-1}^3\right)\right) - f_{4k}^e h_k - \frac{e_k}{6}\hat z_k^3, \quad f_{4k}^e = \frac{1}{2}\sum_{i=1}^{k-1} e_i\left(\hat z_i^2 - \hat z_{i-1}^2\right) - \frac{1}{2}e_k\hat z_k^2, \quad (e \to c)\,.$$

Here $(e \to c)$ means that the similar formulae are valid also for moduli c_k.

Consider the deflection $w(0)$ under action of a harmonic normal pressure $F_3 = F_3^0 \sin r_1 x_1 \sin r_2 x_2$. Then, in Eq. (20)

$$A_1 = A_g - A_\nu - \frac{1}{2}\sum_{k=1}^{n} c_k\left(\hat z_k^2 - \hat z_{k-1}^2\right). \quad (45)$$

According to Remark 2, we have for the second order of accuracy

$$w(0) = w^{\text{KL}}\left(1 - r^2 A_1\right), \quad w^{\text{KL}} = \frac{F_3 h}{Dr^4}, \quad r^2 = r_1^2 + r_2^2, \quad (46)$$

where w^{KL} is deflection in the KL model. In Eqs. (43)–(46) the dimensionless variables (8) are not used and $0 \le z \le h$. We rewrite Eq. (46) as follows:

$$w(0) = w^{\text{KL}}\left(1 - \mu^2 \hat A_1\right), \quad \hat A_1 = \frac{A_1}{h^2}, \quad \mu = rh, \quad (47)$$

where the coefficient $\hat A_1$ is dimensionless.

In the following examples, we put $\mu = 0.2$. For $r_1 = r_2$, this value of μ corresponds to $h/L = 0.045$ where L is the length of the semi-wave in the in-plane directions.

Consider a plate ($n = 4$) with two hard and two soft layers with parameters:

$$h_1 = 0.1,\ h_2 = 0.75,\ h_3 = 0.05,\ h_4 = 0.1,\ E_1 = E_3 = 1,\ E_2 = E_4,\ \nu_1 = \nu_3 = 0.3,\ \nu_2 = \nu_4 = 0.45.$$

The Young's modulus E_2 for the soft layers varies in Table 2.

The exact value $w(0)^{\text{exact}}$ and approximate values w^{KL}, $w^{\text{TR}} = w^{\text{KL}}(1 - \mu^2 \hat A_g)$ and $w(0)^{\text{SA}} = w^{\text{KL}}(1 - \mu^2 \hat A_1)$ are presented in Table 2 for some values of E_2.

We compare the exact and the approximate values of the frequency parameter λ (see (27)). The approximate value is given by Eq. (31),

$$\lambda = \lambda^{\text{KL}}\left(1 - \mu^2\left(\hat A_g - \hat A_\nu - \hat A_\rho\right) + O\left(\mu^4\right)\right)^{-1}, \quad \hat A_g = \frac{A_g}{h^2}, \quad \hat A_\nu = \frac{A_\nu}{h^2}, \quad \hat A_\rho = \frac{A_\rho}{h^2}, \quad (48)$$

Table 3 Errors of the approximate models at the frequency parameter calculation for some values of E_2

E_2	$\lambda^{\text{exact}} \times 10^4$	$\lambda^{\text{KL}} \times 10^4$	$e^{\text{KL}}(\%)$	$\lambda^{\text{TR}} \times 10^4$	$e^{\text{TR}}(\%)$	$\lambda^{\text{SA}} \times 10^4$	$e^{\text{SA}}(\%)$
1	4.930	5.011	1.7	4.943	0.27	4.930	0.006
0.1	1.657	1.735	4.7	1.661	0.27	1.656	0.019
0.01	0.981	1.398	39.3	0.982	0.14	0.980	0.12
0.001	0.303	1.257	314	0.300	0.98	0.300	1.10
0.0001	0.099	1.252	1165	0.038	61.4	0.038	61.4

where for the multi-layered plate A_g and A_ν are the same, cf. Eq. (44),

$$\lambda^{\text{KL}} = \frac{r^4 D}{\langle \rho(z) \rangle}, \quad \langle \rho(z) \rangle = \frac{1}{h} \sum_{k=1}^{n} h_k \rho_k,$$
$$A_\rho = \frac{1}{h} \sum_{k=1}^{n} \left(\rho_k \left(\frac{2 + c_k}{6} \right) \left(\hat{z}_k^3 - \hat{z}_{k-1}^3 \right) - f_{5k} \rho_k h_k + \frac{f_{6k} c_k}{2} \left(\hat{z}_k^2 - \hat{z}_{k-1}^2 \right) \right),$$
$$f_{5k} = \sum_{i=1}^{k-1} \frac{c_i}{2} \left(\hat{z}_i^2 - \hat{z}_{i-1}^2 \right) - \frac{c_k}{2} \hat{z}_k^2, \qquad f_{6k} = \sum_{i=1}^{k-1} h_i \rho_i - \rho_k \hat{z}_k. \tag{49}$$

Let us consider a plate with the same parameters and assume additionally that $\rho_1 = \rho_3 = 1$, $\rho_2 = \rho_4 = 0.2$. Table 3 presents the exact values λ^{exact} and the approximate values λ^{KL} for some values of E_2. $\lambda^{\text{TR}} = \lambda^{\text{KL}}(1 - \mu^2 \hat{A}_g)^{-1}$ and $\lambda^{\text{SA}} = \lambda^{\text{KL}}(1 - \mu^2(\hat{A}_g - \hat{A}_\nu - \hat{A}_\rho))^{-1}$.

The conclusions from Tables 2 and 3 are the same and presented in the following.

For the small level of heterogeneity ($E_2 \sim$ 1–0.1), the accuracy of the KL model is sufficient for applications and the SA model leads to a very small error of order 10^{-4}–10^{-5}. For example, such a high level of accuracy is necessary in manufacturing of flexible telescope mirrors. The TR model is slightly more exact than the KL model.

For a large level of heterogeneity ($E_2 \sim 0.01$–0.001), the KL model is unacceptable and both models (TR and SA) lead to similar errors of the order 1% which is acceptable for practical applications. For this level of heterogeneity, it is possible to use the generalized TR model for the simplification of calculations (see Sect. 7). In this case, it is necessary to determine only coefficient A_g and avoid calculation of the bulk coefficients A_ν and A_ρ.

The available 2D models are not applicable for essential heterogeneity $E_2 \sim 0.0001$.

7 Generalized Timoshenko–Reissner model

In contrast to the KL model, the TR model for a homogeneous transversally isotropic plate involves the transversal shear strains [3,4]

$$\varepsilon_{i3} = \frac{\partial u_i}{\partial x_3} + \frac{\partial u_3}{\partial x_i} = \frac{5}{4} \left(1 - \frac{4z^2}{h^2} \right) \gamma_i \left(x_1, x_2 \right), \quad i = 1, 2, \tag{50}$$

where γ_i denotes the average transversal shear angle. From this assumption and the assumption that $\sigma_{33} = 0$, we obtain the following relations of 2D elasticity:

$$M_{11} = D(\kappa_1 + \nu \kappa_2), \quad M_{22} = D(\kappa_2 + \nu \kappa_1), \quad M_{12} = (1 - \nu) D \tau,$$
$$Q_1 = \Gamma \gamma_1, \quad Q_2 = \Gamma \gamma_2, \qquad \Gamma = \frac{5}{6} G_{13} h, \quad D = \frac{E h^3}{12 \left(1 - \nu^2 \right)}, \tag{51}$$

where M_{11}, M_{22} are the bending moments, M_{12} is the torque, Q_1, Q_2 are the transversal stress resultants and

$$\kappa_1 = \frac{\partial \varphi_1}{\partial x_1}, \quad \kappa_2 = \frac{\partial \varphi_2}{\partial x_2}, \quad 2\tau = \frac{\partial \varphi_1}{\partial x_2} + \frac{\partial \varphi_2}{\partial x_1},$$
$$\varphi_1 = \gamma_1 - \frac{\partial w}{\partial x_1}, \quad \varphi_2 = \gamma_2 - \frac{\partial w}{\partial x_2}, \tag{52}$$

and φ_i stands for the average angle of rotation of a normal fibre.

The 2D equilibrium equations are as follows:

$$\frac{\partial M_{11}}{\partial x_1} + \frac{\partial M_{12}}{\partial x_2} - Q_1 - J\frac{\partial^2 \varphi_1}{\partial t^2} + m_1 = 0,$$
$$\frac{\partial M_{12}}{\partial x_1} + \frac{\partial M_{22}}{\partial x_2} - Q_2 - J\frac{\partial^2 \varphi_2}{\partial t^2} + m_2 = 0, \quad J = \frac{\rho h^3}{12},$$
$$\frac{\partial Q_1}{\partial x_1} + \frac{\partial Q_2}{\partial x_2} - \rho h\frac{\partial^2 w}{\partial t^2} + F_3 = 0. \tag{53}$$

Equations (51)–(53) can be used also for heterogeneous transversally isotropic plates if we take the proper values of the equivalent parameters

$$D = D_{\text{eq}}, \quad \rho = \rho_{\text{eq}}, \quad J = J_{\text{eq}}, \quad \Gamma = \Gamma_{\text{eq}}. \tag{54}$$

As we will show in what follows, the first three parameters (54) can be found within the framework of the KL hypothesis about the straight normal. Also, in order to find Γ_{eq} it is necessary to use asymptotic expansions of Sect. 3.

We compare the results from Eqs. (51)–(53) with parameters (54) and the results of Sects. 3 and 4. For this aim, we analyse Eqs. (51)–(53). In this system, the principal unknown quantities are w, γ_1, γ_2 or w, φ_1, φ_2. Instead of φ_1, φ_2, we introduce the new unknown quantities Ψ and Θ by the relations

$$\varphi_1 = -\frac{\partial \Psi}{\partial x_1} + \frac{\partial \Theta}{\partial x_2},$$
$$\varphi_2 = -\frac{\partial \Psi}{\partial x_2} - \frac{\partial \Theta}{\partial x_1}. \tag{55}$$

Now, for a transversely isotropic plate, the 2D system (51) (similar to the 3D system given by Eq. (1)) is split into the equation

$$\frac{1-\nu}{2} D\Delta^2\Theta - \Gamma\Delta\Theta - J\frac{\partial^2 \Delta\Theta}{\partial t^2} - \frac{\partial m_1}{\partial x_2} + \frac{\partial m_2}{\partial x_1} = 0 \tag{56}$$

and the system

$$\Gamma(\Delta w - \Delta\Psi) - \rho h\frac{\partial^2 w}{\partial t^2} + F_3 = 0,$$
$$-D\Delta^2\Psi - \rho h\frac{\partial^2 w}{\partial t^2} + J\frac{\partial^2 \Delta\psi}{\partial t^2} + F_3 + \frac{\partial m_1}{\partial x_1} + \frac{\partial m_2}{\partial x_2} = 0. \tag{57}$$

Equation (56) describes the boundary layers and is beyond the scope of the present paper. Equation (57) reduces to the equation of fourth order for deflection $w(x_1, x_2)$

$$D\Delta^2 w + \rho h\frac{\partial^2 w}{\partial t^2} - \left(\frac{D\rho h}{\Gamma} + J\right)\frac{\partial^2 \Delta w}{\partial t^2} + \frac{J\rho h}{\Gamma}\frac{\partial^4 w}{\partial t^4} - F_3 + \frac{D}{\Gamma}\Delta F_3 - \frac{J}{\Gamma}\frac{\partial F_3}{\partial t^2} - \frac{\partial m_1}{\partial x_1} - \frac{\partial m_2}{\partial x_2} = 0. \tag{58}$$

We compare Eq. (58) with more exact equations in statics and in dynamics (free vibration).

Static case In the static case, Eq. (58) gives

$$D_{\text{eq}}\Delta^2 w = F_3 - \frac{D_{\text{eq}}}{\Gamma_{\text{eq}}}\Delta F_3 + \frac{\partial m_1}{\partial x_1} + \frac{\partial m_2}{\partial x_2}. \tag{59}$$

We compare this equation with Eq. (18) (in dimensionless form):

$$D\mu^4\Delta^2 w(0) = F_3 + \mu^2 A_g \Delta F_3 - \mu^2 A_\nu \Delta F_3 + \mu^2 L(\Delta f_3) - \mu^2 M \tag{60}$$

At first, we note that in the TR model $w(z) = \text{const.}$, and Eq. (59) does not describe small Poisson effects related to the summands $-\mu^2 A_\nu \Delta F_3$ and $L(\Delta f_3)$ in Eq. (60). By choosing D_{eq} and Γ_{eq}, the following relation between the summands of Eqs. (59) and (60) can be established:

$$D_{\text{eq}} = E_* \int_0^h (z-a)^2 c_0(z)\mathrm{d}z, \quad a = \int_0^h c_0(z)\mathrm{d}z, \quad E_* = \frac{1}{h}\int_0^h E_0(z)\mathrm{d}z, \quad c_0 = \frac{E_0(z)}{E_*},$$
$$\frac{1}{\Gamma_{\text{eq}}} = \frac{E_*}{D_{\text{eq}}^2}\int_0^h c_0(z)(z-a)\int_0^z c_g(z_1)\int_0^{z_1} c_0(z_2)(z_2-a)\mathrm{d}z_2\mathrm{d}z_1\mathrm{d}z, \qquad c_g(z) = \frac{E_*}{G_{13}(z)}. \tag{61}$$

For the harmonic compression F_3, the error of the generalized TR model can be estimated by comparison with the columns w^{TR} and w^{exact} in Tables 1 and 2.

Free vibrations We consider the free vibrations of natural frequency ω and with the harmonic vibration mode $w(x_1, x_2) = w^0 \sin r_1 x_1 \sin r_2 x_2$. Equation (58) yields the quadratic equation for ω^2,

$$D_{\text{eq}} r^4 - \rho_{\text{eq}} h\omega^2 - \left(\frac{D_{\text{eq}}\rho_{\text{eq}} h}{\Gamma_{\text{eq}}} + J_{\text{eq}}\right) r^2\omega^2 + \Omega_4 = 0, \quad \Omega_4 = \frac{J_{\text{eq}}\rho_{\text{eq}} h}{\Gamma_{\text{eq}}}\omega^4 = 0, \qquad r^2 = r_1^2 + r_2^2. \tag{62}$$

We compare this equation with the asymptotic dimensionless equation (see Eq. (31)),

$$D\mu^4 = \lambda\left(1 - \mu^2(A_g - A_\nu - A_\rho)\right), \quad \lambda = \frac{\rho_* h^2\omega^2}{E_*}, \quad \mu = rh, \tag{63}$$

with

$$A_\rho = \int_0^1 (z-a)^2\rho_0(z)\mathrm{d}z + \int_0^1 \left(c_\nu(z)(z-a)\int_0^z \rho_0(z_1)\mathrm{d}z_1 - \rho_0(z)\int_0^z c_\nu(z_1)(z_1-a)\mathrm{d}z_1\right)dz. \tag{64}$$

By means of Eq. (54), a relation between Eqs. (62) and (63) can be established.

We take the same values (61) for D_{eq} and Γ_{eq}, assume $\rho_{\text{eq}} = \rho_*$, and obtain

$$J_{\text{eq}} = \int_0^1 (z-a)^2\rho(z)\mathrm{d}z\mathrm{d}z. \tag{65}$$

As in the static case, the summands with A_ν and $c_\nu(z)$ are not contained in Eq. (62). This equation involves the additional summand Ω_4 which is very small for the studied low-frequency vibration and can be omitted. This summand describes the second (high-frequency) branch of the curve $\lambda(\mu)$ [8,38].

For low-frequency vibration of the multi-layered plate, the error of the generalized TR model can be estimated by comparison with the columns λ^{TR} and λ^{exact} in Table 3.

For orthotropic beams and for transversally isotropic plates, the generalized TR model is discussed in details in [43], and Refs. [44–47] reported some applications.

8 Deflection and free vibrations of a rectangular heterogeneous plate

Consider a rectangular plate with $0 \le x_1 \le a_1,\ 0 \le x_2 \le a_2,\ 0 \le z \le h$ (Fig. 4). In the previous sections, the boundary conditions at a plate edges were not prescribed or a plate was assumed to be infinite in the in-plane directions. Now the following variant of boundary conditions is assumed:

$$\begin{aligned} u_2 = w = \sigma_{11} = 0 \quad &\text{at} \quad x_1 = 0, \quad x_1 = a_1, \\ u_1 = w = \sigma_{22} = 0 \quad &\text{at} \quad x_2 = 0, \quad x_2 = a_2, \end{aligned} \tag{66}$$

(the so-called Navier conditions) and

$$\sigma_{13} = \sigma_{23} = 0,\ \sigma_{33} = -F_3^0 \quad \text{at} \quad z = 0; \qquad \sigma_{13} = \sigma_{23} = \sigma_{33} = 0 \quad \text{at} \quad z = h. \tag{67}$$

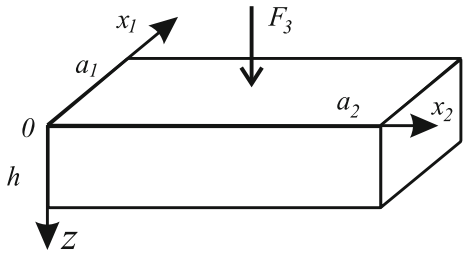

Fig. 4 Plate under consideration

As in Sect. 2 [see Eq. (4)], we replace the condition $\sigma_{33}(x_1, x_2, 0) = -F_3^0$ by $\sigma_{33}(x_1, x_2, 0) = 0$ and take $f_3(x_1, x_2, z) = F_3^0\delta(z)$, where $\delta(z)$ is the Dirac delta function.

The functions

$$\begin{aligned} u_1(x_1, x_2, z) &= r_{1m}\, u(z) \cos(r_{1m}x_1) \sin(r_{2n}x_2), \\ u_2(x_1, x_2, z) &= r_{2n}\, u(z) \sin(r_{1m}x_1) \cos(r_{2n}x_2), \quad r_{1m} = \frac{m\pi}{a_1},\ r_{2n} = \frac{n\pi}{a_2}, \quad m, n = 1, 2, \ldots, \\ w(x_1, x_2, z) &= w(z) \sin(r_{1m}x_1) \sin(r_{2n}x_2) \end{aligned} \tag{68}$$

satisfy the boundary conditions (66). The boundary layer does not appear, because $v = \partial u_2/\partial x_1 - \partial u_1/\partial x_2 \equiv 0$ [see Eq. (5)].

We assume the harmonic load $f_3(x_1, x_2, z) = f_3^0(z) \sin r_1 x_1 \sin r_2 x_2$ and follow Remark 2, that is, we replace Δ by -1 and take $\mu = h/L$, $L = (r_1^2 + r_2^2)^{-1/2}$); then, system (9) becomes a system of ODE which can be solved numerically by the Runge–Kutta method.

We expand force F_3^0 in a double Fourier series

$$F_3^0 = F_3^0 \sum_{m,n=1,3,\ldots} \frac{16}{mn\pi^2} \sin(r_{1m}x_1) \sin(r_{2n}x_2), \tag{69}$$

and apply Eqs. (9) to each summand of (69) for

$$\mu = \mu_{mn} = h\, \left(r_{1m}^2 + r_{2n}^2\right)^{1/2}. \tag{70}$$

We consider the multi-layered plate studied in Sect. 6. The exact solution of the studied problem can be presented as a convergent series:

$$w(x_1, x_2, z) = F_3^0 \sum_{m,n=1,3,\ldots} \frac{16}{mn\pi^2}\, w_{nm}(z) \sin(r_{1m}x_1) \sin(r_{2n}x_2), \tag{71}$$

where $w_{mn}(z)$ is the solution of Eq. (9) (transformed according to Remark 2) with the boundary conditions

$$\sigma_{33}(0) = -1, \qquad \sigma(0) = \sigma(h) = \sigma_{33}(h) = 0. \tag{72}$$

The approximate deflection of the plane $z = 0$ can be found by using the results of Sect. 6, and it reads as:

$$w(x_1, x_2, 0) = \frac{F_3^0}{D} \sum_{m,n=1,3,\ldots} C_{mn} \sin(r_{1m}x_1) \sin(r_{2n}x_2), \qquad C_{mn} = \frac{16\left(1 - \mu_{mn}^2 A_1\right)}{mn\pi^2 \mu_{mn}^4}, \tag{73}$$

where D and A_1 are given in Eqs. (44) and (45), respectively. The similar expression is valid for the deflection of the face plane $w(x_1, x_2, h)$. In this case, constant A_1 in Eq. (70) is to be replaced by $A = A_g - A_v$.

The deflection of the line $x_2 = a_2/2$, $z = 0$ and the maximal deflection at $z = 0$ are, respectively,

$$w(x_1, a_2/2, 0) = \frac{F_3}{D} \sum_{k=0}^{\infty} B_{2k+1} \sin\left(r_{1,2k+1}x_1\right), \quad B_{2k+1} = \sum_{j=0}^{\infty} (-1)^j\, C_{2k+1,2j+1},$$

Table 4 Coefficients $C_{2k+1,2j+1}$, B_{2k+1}, and A_0 for various values E_2

E_2	C_{11}	$C_{13}=C_{31}$	C_{33}	$C_{15}=C_{51}$	$C_{35}=C_{53}$	C_{55}	B_1	B_3	B_5	A_0
1	1594	24	3	3	1	0	1573	21	2	1555
0.1	4877	86	11	11	3	1	4802	76	9	4735
0.01	9897	343	57	68	17	7	9622	303	58	9380
0.001	45,787	2723	498	617	157	64	43,562	2383	524	41,703

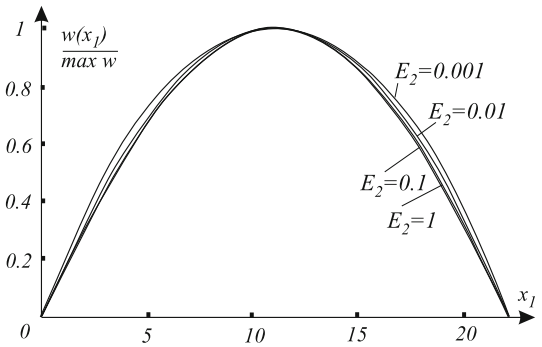

Fig. 5 Deflection modes for various values of the Young moduli ratio E_2

$$w\,(a_1/2, a_2/2, 0) = \frac{F_3}{D} A_0, \quad A_0 = \sum_{k,j=0}^{\infty} (-1)^{k+j} C_{2k+1,2j+1}. \tag{74}$$

The series in Eq. (74) converge rapidly, and the summand with C_{11} is much larger than the remaining summands (see Table 4).

As an example, we consider a multi-layer square plate with the same values of parameters as in Sect. 6. We additionally assume that $a_1 = a_2 = 22.2$, which corresponds to $\mu = 0.2$. For various values E_2, the first coefficients $C_{2k+1,2j+1}$, B_{2k+1}, and A_0 are given in Table 4.

The amplitude of deflection is proportional to A_0 and essentially depends on ratio E_2 of the Young's moduli (see Table 4), but the deflection mode weakly depends on E_2 and is close to function $\sin(\pi x_1/a)$ (see Fig. 5).

The accuracy of the approximate solution (73) depends upon how exact coefficients C_{mn} are determined. This can be established by a comparison with the exact solution (71). These calculations are not fulfilled, but for free vibrations the relative errors

$$e_{mn} = \frac{\lambda^a_{mn} - \lambda^{\text{exact}}_{mn}}{\lambda^a_{mn}} \cdot 100\% \tag{75}$$

of the approximate values λ_{mn} of the frequency parameter λ are given in Table 5. As it follows from a comparison of Tables 2 and 3, the errors for the deflections and for the frequency parameters are close to each other. Finally, we note that the error grows simultaneously with the increase in numbers m and n and with increase in the level of heterogeneity E_2^{-1}.

We consider free vibrations of a rectangular plate with $0 \le x_1 \le a_1,\ 0 \le x_2 \le a_2,\ 0 \le z \le h$, satisfying the boundary conditions (66) and (4). A two-parametric set of vibration modes is given by Eqs. (68). The exact frequency parameter $\lambda^{\text{exact}}_{mn}$ can be found numerically from Eqs. (9),(26) by taking $\mu^2 = \mu^2_{mn}$ as in Eq. (70).

The approximate expression (48) for the long-wave low-frequency vibrations gives

$$\lambda^a_{mn} = \frac{D\mu^4_{mn}}{\langle\rho\rangle} \left(1 - \mu^2_{mn}(A_g - A_\nu - A_\rho)\right)^{-1}, \qquad m, n = 1, 2, \ldots \tag{76}$$

The results of comparison of the exact $\lambda^{\text{exact}}_{mn}$ and the approximate λ^a_{mn} values of the frequency parameter λ for the plate parameters of Sect. 6 are given in Table 5. For a fixed value of E_2, the error increases with numbers m and n because the small parameter μ_{mn} grows. Therefore, only a few first values λ^a_{mn} can be determined by using Eq. (76).

For the boundary conditions, different from (66), the analytical solution of the problems studied in this Section is essentially more difficult, because solution (68) is to be changed, and additionally the edge effects and the boundary layers can appear.

Table 5 Relative error e_{mn} of the approximate values λ_{mn}

E_2	$(mn) = (11)$	(12)	(22)	(13)	(23)	(33)	(15)	(35)	(55)
	$\mu_{mn} = 0.20$	0.32	0.40	0.45	0.51	0.60	0.72	0.82	1.00
	e_{11}	e_{12}	e_{22}	e_{13}	e_{23}	e_{33}	e_{15}	e_{35}	e_{55}
1	0.0	0.0	0.1	0.1	0.2	0.4	0.7	1.0	1.8
0.1	0.0	0.1	0.2	0.3	0.5	0.8	1.4	1.9	2.8
0.01	0.1	0.4	0.8	1.1	1.2	1.6	2.2	2.8	3.8
0.001	1.1	2.9	4.7	5.9	6.7	10.3	14.3	18.0	25.4

9 Conclusions

A two-dimensional linear model of second-order accuracy (SA), describing a bending of a thin plate made of transversally isotropic heterogeneous material is considered. The suggested algorithm has been announced in the short paper [7] for the static case. The SA model can be applied for functionally gradient materials and for multi-layer plates. The SA model describes both the plate deflection and the lower branch of a curve $\lambda(\mu)$.

The range of anisotropy and variability of elastic moduli in the thickness direction (described by the shear parameter $g = \mu^2 E/G$) at which the SA model gives acceptable results is investigated. It is proved that this range is very broad.

The accuracy of the SA model is very high for problems with small g ($g \ll 1$), namely for sufficiently thin plates made of materials close to isotropic homogeneous. In this case, the SA model gives essentially more exact results than the KL and the TR models.

The accuracy of all models, namely the KL, the TR, and the SA models, decreases with increasing g.

For problems with large g, $g \sim 1$, the KL model is inacceptable. The generalized TR model, in which a multi-layer heterogeneous plate is replaced by a one-layered homogeneous transversely isotropic plate with some equivalent parameters, is proposed. It is important to note that the accuracy of the generalized TR model is close to the accuracy of the SA model; however, the generalized TR model is simpler for calculations than the SA model.

For problems with very large g, $g \gg 1$, the studied 2D models are inacceptable.

For the Navier boundary conditions, the deflection and free vibration of a rectangular heterogeneous plate are studied in detail.

Acknowledgements The work is supported by Russian Foundation for Basic Research, Grants 16-01-00580-a and 16-51-52025 MNT-a.

References

1. Kirchhoff, G.: Vorlesungen über mathematische Physik. Mechanik, Leipzig (1876). [in German]
2. Love, A.E.H.: A Treatise on the Mathematical Theory Elasticity. Cambridge University Press, Cambridge (1927)
3. Timoshenko, S.P.: On the correction for shear of the differential equation for transverse vibrations of prismatic bars. Philos. Mag. **41**, 744–746 (1921)
4. Reissner, E.: The effect of transverse shear deformation on the bending of elastic plates. Trans. ASME J. Appl. Mech. **12**, 69–77 (1945)
5. Chernykh, K.F., Rodionova, V.A., Titaev, B.F.: Applied Theory of Anisotropic Plates and Shells. St.Petersburg University Press, Saint Petersburg (1996). [in Russian]
6. Goldenweizer, A.L.: Theory of Elastic Thin Shells. Pergamon Press, Oxford (1961)
7. Tovstik, P.E., Tovstik, T.P.: A thin-plate bending equation of second-order accuracy. Dokl. Phys. **59**(8), 389–392 (2014)
8. Tovstik, P.E.: On the asymptotic character of approximate models of beams, plates and shells, Vestnik St.Petersburg Univ. Mathematics. Allerton Press, NewYork **3**, 49–54 (2007)
9. Vetyukov, Y., Kuzin, A., Krommer, M.: Asymptotic splitting in the three-dimensional problem of elasticity for non-homogeneous piezoelectric plates. Int. J. Solids Struct. **48**, 12–23 (2011)
10. Eremeev, V.A., Zubov, L.M.: Mechanics of Elastic Shells. Nauka, Moscow (2008). [in Russian]
11. Altenbach, H., Mikhasev, G.I. (eds.): Shell and Membrane Theories in Mechanics and Biology. Springer, Berlin (2014)
12. Tovstik, P.E., Tovstik, T.P.: Two-dimensional model of anisotropic of shells. Shell structures: theory and Applications. Proceedings of the 10th SSTA 2013 Conference, 3, 153–156 (2014)
13. Andrianov, I.V., Danishevskyy, V.V., Weichert, D.: Boundary layers in fibrous composite materials. Acta Mech. **216**, 3–15 (2011)
14. Tovstik, P.E., Tovstik, T.P.: On the 2D models of plates and shells including shear. ZAMM. **87**(2), 160–171 (2007)

15. Tovstik, P.E., Tovstik, T.P.: Two-dimensional linear model of elastic shell accounting for general anisotropy of material. Acta Mech. **225**(3), 647–661 (2014)
16. Tovstik, P.E.: Two-dimensional models of plates made of an anisotropic material. Dokl. Phy. **54**(4), 205–209 (2009)
17. Tovstik, P.E., Tovstik, T.P.: Two-dimensional model of plate made of anisotropic inhomogeneous material. Proceedings of the ICNAAM-2014. AIP Conf. Proc. 1648, art. no.300011 (2015)
18. Birman, V.: Plate structures. Solid mechanics and its applications, vol. 178. Springer, Netherlands (2011)
19. Grossi, R.O.: Boundary value problems for anisotropic plates with internal line hinges. Acta Mech. **223**(1), 125–144 (2011)
20. Reddy, J.N.: A refined nonlinear theory of plates with transvere shear deformation. Int. J. Solids and Struct. **20**, 881–896 (1894)
21. Bauer, S., Voronkova, E.: Nonclassical theories of bending analysis of orthotropic circular plate. Shell structures theory and application Proceedings of the 10th SSTA 2013 Conference V. 3, 57–60 (2014)
22. Reddy, J., Wang, C.: An overview of the relationship between the classical and shear deformation plate theories. Compos. Sci. Technol. **60**, 2327–2335 (2000)
23. Barretta, R.: Analogies between Kirchhoff plates and Saint-Venant beams under flexure. Acta Mech. **225**(7), 2075–2083 (2014)
24. Batista, M.: An exact theory of the bending of transversely inextensible elastic plates. Acta Mech. **226**(9), 2899–2924 (2015)
25. Zhang, G.Y., Gao, X.-L., Wang, J.Z.: A non-classical model for circular Kirchhoff plates incorporating microstructure and surface energy effects. Acta Mech. **226**(12), 4073–4085 (2015)
26. Donnell, L.H.: Beams, Plates and Shells. McGraw-Hill, NewYork (1976)
27. Timoshenko, S.P.: Strength of Materials. Van Vistrand, New York (1956)
28. Ambartsumjan, S.A.: Theory of anisotropic shells. Progress in Materias Science. Ser. II. Stanford, Conn.: Technomic (1970)
29. Jawad, M.H.: Theory and Design of Plate and Shell Structures. Springer, Berlin (1994)
30. Altenbach, H.: Theories of laminated and sandwich plates. Overv. Mech. Compos. Mater. **34**, 333–349 (1998)
31. Eremeev, V.A., Ivanova, E.A., Altenbach, H., Morozov, N.F.: On effective stiffness of a three-layered plate with a core filled with a capillary fluid. Shell structures theory and application Proceedings of the 10th SSTA 2013 Conference. Vol. 3, 85–88 (2014)
32. Morozov, N.F., Tovstik, P.E.: Bending of two-layer beam with non-rigid contact between layers. Appl. Math. and Mech. **75**, 77–84 (2011)
33. Reddy, J.N.: Mechanics of Laminated Composite Plates and Shells. CRC, Boca Raton (2004)
34. Aghalovyan, L.A.: On the classes of problems for deformable one-layer and multilayer thin bodies solvable by the asymptotic method. Mech. Compos. Mater. **47**(1), 59–72 (2011)
35. Asnafi, A., Abedi, M.: A complete analogical study on the dynamic stability analysis of isotropic functionally graded plates subjected to lateral stochastic loads. Acta Mech. **226**(7), 2347–2363 (2015)
36. Tovstik, P.E., Tovstik, T.P.: Free vibrations of anisotropic beam. Vestnik St.Peterdurg Univ. Ser. 1,**1**(59), 4, 599–608 (2014)
37. Goldenweizer, A.L., Lidsky, V.B., Tovstik, P.E.: Free Vibrations of Thin Elastic Shells. Nauka, Moscow (1979). [in Russian]
38. Tovstik, P.E.: Vibrations and stability of a prestressed plate on an elastic foundation. Appl. Math. Mech. **73**(1), 77–87 (2009)
39. Grossi, R.O., Raffo, J.: Natural vibrations of anisotropic plates with several internal line hinges. Acta Mech. **224**(11), 2677–2697 (2014)
40. Sarangi, S.K., Ray, M.C.: Active damping of geometrically nonlinear vibrations of laminated composite plates using vertically reinforced 1–3 piezoelectric composites. Acta Mech. **222**(3–4), 363–380 (2011)
41. Morozov, N.F., Tovstik, P.E.: On chessboard buckling modes in compressed materials. Acta Mech. **223**, 1769–1776 (2012)
42. Kienzler, R., Schneider, P.: Comparison of various linear plate theories in the light of a consistent second order approximation. Shell structures theory and application. Proceedings of the 10th SSTA 2013 Conference V. 3, 109–112 (2014)
43. Tovstik, P.E., Tovstik, T.P.: Generalized Timoshenko-Reissner models for beams and plates, strongly heterogeneous in the thickness direction. ZAMM (2016). doi:10.1002/zamm.201600052
44. Morozov N.F., Tovstik, P.E., Tovstik, T.P.: Generalized Timoshenko–Reissner model for a multilayer plate. Mech. Solids **51**, 527–537 (2016)
45. Morozov, N.F., Tovstik, P.E., Tovstik, T.P.: The Timoshenko-Reissner generalized model of a plate highly nonuniform in thickness. Dokl. Phys. **61**(8), 394–398 (2016)
46. Morozov N.F., Tovstik P.E., Tovstik T.P.: Continuum model of multilowered nano-plate. Dokl. Phys. **61**(11), 567–570 (2016)
47. Tovstik, P.E., Tovstik, T.M.: Bending stiffness of a multilayered plate // ECCOMAS Congress 2016 - Proceedings of the 7th European Congress on Computational Methods in Applied Sciences and Engineering. **3**, Pages 3423–3435 (2016)
48. Berdichevsky, V.L.: An asymptotic theory of sandwich plates. Int. J. of Eng. Sci. (2009). doi:10.1016/j.ij.engsci.2009.09.001